

**Evaporative Controls on Convective Adjustment: A Satellite-Based
Assessment of Convective Available Energy (CAPE) During Surface
Drydowns**

by

Lily N. Zhang

Submitted to the Department of Earth, Atmospheric and Planetary Sciences

in Partial Fulfillment of the Requirements for the Degree of

Bachelor of Science in Earth, Atmospheric and Planetary Sciences

at the Massachusetts Institute of Technology

May 6, 2022

Copyright 2022 Lily N. Zhang. All rights reserved.

The author hereby grants to MIT permission to reproduce
and to distribute publicly paper and electronic copies of this
thesis document in whole or in part in any medium now
known or hereafter created.

Author _____
Department of Earth, Atmospheric and Planetary Sciences
May 6, 2022

Certified by _____
Dara Entekhabi
Thesis Supervisor

Accepted by _____
Thomas Herring
Chair, Committee on Undergraduate Program

Evaporative Controls on Convective Adjustment: A Satellite-Based Assessment of Convective Available Energy (CAPE) During Surface Drydowns

by

Lily N. Zhang

Submitted to the Department of Earth, Atmospheric and Planetary Sciences
in Partial Fulfillment of the Requirements for the Degree of
Bachelor of Science in Earth, Atmospheric and Planetary Sciences

ABSTRACT

Changes in surface properties are known to influence weather and climate through interactions between the land and atmosphere. In convective atmospheres, convective available potential energy (CAPE) drives convective adjustment and can lead to precipitation. We study the evolution of CAPE during drydowns, interstorm periods over which evapotranspiration occurs, to understand the impact of evaporative controls on convective adjustment. Our results show that drydown CAPE development varies geographically based on hydroclimate and can also depend on initial soil moisture content and moist enthalpy conditions. The impact of these factors on CAPE can be explained by their effect on evaporation, demonstrating the importance of evaporative controls on convective adjustment and providing a benchmark for understanding the relationship between soil moisture and precipitation.

ACKNOWLEDGMENTS

This project would not have been possible without the guidance and insight of Professor Dara Entekhabi, who I also credit for introducing me to the topic of land-atmosphere interactions last spring. I would also like to thank Entekhabi group members Dan Gianotti and Jianzhi Dong for their time and valuable contributions.

I am grateful to Professor Susan Solomon, Professor Kerry Emanuel, and Dr. Ryan Woosley for being the most wonderful mentors I could ever ask for, as well as to the rest of the PAOC community for supporting me in my time at EAPS.

Lastly, I would like to dedicate this thesis to my father, who unfortunately could not be here to see me complete my degree but has and continues to inspire me endlessly.

CONTENTS

Tables and Figures	5
1 Introduction	6
2 Methods	9
2.1 Data Sets	9
2.1.1 <i>Soil Moisture</i>	9
2.1.2 <i>Meteorological Data</i>	9
2.2 Data Processing	10
2.2.1 <i>CAPE and Moist Enthalpy Calculations</i>	10
2.2.2 <i>SMAP Regridding</i>	10
2.2.3 <i>Drydown Identification</i>	11
2.3.4 <i>Warm Season Definition</i>	12
2.4 Drydown Day Zero Maps	13
3 Continental US Focus Area	15
3.1 Western and Eastern US Comparison	15
3.2 “Tagging” by Initial Conditions	17
3.2.1 <i>Initial Soil Moisture Comparison</i>	18
3.2.2 <i>Initial Moist Enthalpy Comparison</i>	20
3.3 Discussion	22
4 Global Patterns	24
4.1 Summary Statistics	24
4.2 Results	24
4.2.1 <i>Soil Moisture Tag</i>	26
4.2.2 <i>Moist Enthalpy Tag</i>	28
4.2.3 <i>Sensible and Latent Heat Tags</i>	30
4.3 Discussion	31
4.3.1 <i>Geographical Trends</i>	31
4.3.2 <i>Soil Moisture’s Impact</i>	32
4.3.3 <i>Understanding the Moist Enthalpy Tag</i>	32
5 Conclusion	34
References	36

TABLES AND FIGURES

Figure 1. Drydown time scales.	12
Figure 2. Initial drydown CAPE.	13
Figure 3. Initial drydown moist enthalpy, sensible heat, and latent heat.	14
Figure 4. Average CAPE and Δ CAPE/day over CONUS.	15
Figure 5. Time series of drydown CAPE over Eastern and Western US.	16
Figure 6. Time series of drydown soil moisture, moist enthalpy, sensible heat, and latent heat over Eastern and Western US.	17
Figure 7. Time series of drydown CAPE over Eastern and Western US, tagged by soil moisture.	18
Figure 8. Time series of drydown soil moisture, moist enthalpy, sensible heat, and latent heat over Eastern and Western US, tagged by soil moisture.	19
Figure 9. Time series of drydown CAPE over Eastern and Western US, tagged by moist enthalpy.	20
Figure 10. Time series of drydown soil moisture, moist enthalpy, sensible heat, and latent heat over Eastern and Western US, tagged by moist enthalpy.	21
Figure 11. Mean and percent positive Δ CAPE/day map.	24
Figure 12. Mean and percent positive Δ ME/day, $\Delta c_p T$ /day and ΔLq /day map.	25
Figure 13. Mean and percent positive Δ CAPE/day map, tagged by soil moisture.	26
Figure 14. Mean and percent positive Δ ME/day, $\Delta c_p T$ /day and ΔLq /day map, tagged by soil moisture.	27
Figure 15. Mean and percent positive Δ CAPE/day map, tagged by moist enthalpy.	28
Figure 16. Mean and percent positive Δ ME/day, $\Delta c_p T$ /day and ΔLq /day map, tagged by moist enthalpy,	29
Figure 17. Mean and percent positive Δ CAPE/day map, tagged by sensible heat and latent heat.	30
Figure 18. Mean and percent positive Δ ME/day map, tagged by sensible heat and latent heat.	31

1 Introduction

Coupling between the land surface and atmosphere is known to impact both weather and climate and has increasingly become a topic of interest in the modeling community. Soil moisture, in particular, plays an important role in land atmosphere coupling by moderating energy fluxes and evaporation at the surface. Modeling and observation-based studies suggest a relationship between soil moisture and precipitation, but with inconsistent results (Seneviratne et al., 2010). Disagreement between observational studies can largely be attributed to the scarcity of soil moisture observations and difficulties of establishing statistical causality within the available data (Seneviratne et al., 2010; Salvucci et al., 2002). Even amongst modeling studies, however, we see a range of suggested feedbacks (Koster et al., 2004; Tuttle and Salvucci, 2016).

Intrinsically, the soil moisture-precipitation relationship is difficult to characterize because it is the result of multiple processes occurring both in the atmosphere and at the surface. Depending on factors such as regional climate, the relative importance of each process and the interactions between them may differ. Because of the complex nature of the soil moisture-precipitation relationship, we choose to focus on a specific pathway for precipitation, convection, and explore its relationship with soil moisture using theory and observations.

In convecting atmospheres, warm parcels of air rise from the surface up through the colder, denser atmosphere. As the parcels cool, the water vapor within them

may condense and produce convective precipitation. The amount of energy available for convection can be quantified in terms of the convective available potential energy (CAPE). CAPE is an important component of the atmospheric energy budget and drives convective adjustments on short time scales (Emanuel, 1994). High values of CAPE indicate an unstable atmosphere with a lot of upwards motion. In extreme cases, this can produce severe weather events such as tornadoes and thunderstorms.

Emanuel (1994) found that the time rate of change in CAPE for a parcel i could be approximated as:

$$\frac{\partial}{\partial \tau} CAPE_i \cong (T_i - T_{LNB_i}) \frac{\partial s_i}{\partial \tau} - \int_{z_i}^{z_{LNB_i}} \left(\frac{g\dot{Q}}{c_p T} - \frac{g}{\theta} \mathbf{V}_r \cdot \Delta\theta - N^2 \omega \right) dz \quad (1)$$

where changes in CAPE are the result of radiative cooling (\dot{Q}), horizontal convergence of heat ($\Delta\theta$), vertical transport (N), and changes in the parcel's entropy ($\frac{\partial s_i}{\partial \tau}$). Changes in entropy are related to evaporation through the following relationship:

$$\frac{\partial s_i}{\partial \tau} \sim \frac{C_D L_v |\mathbf{V}_a| (r_s^* - r_b)}{T_i \Delta z_b} \sim \frac{Evaporation}{T_i \Delta z_b} \quad (2)$$

Key here to our study is that increases in CAPE are driven by increases in parcel entropy (s_i) which, in turn, is increased through surface evaporation. Simply put, increases in CAPE over time are driven by surface evaporation. This relationship between CAPE and evaporation serves as the foundation for our

study of CAPE evolution over interstorm periods and provides a theoretical basis for the relationship between soil moisture and precipitation.

In our study, we focus on CAPE development during surface drydowns, interstorm periods over which evapotranspiration occurs. During a drydown, soil moisture consistently decreases as evaporation takes place without the influence of precipitation (McColl et al., 2017). We take drydowns to be a fundamental unit of time for land-atmosphere interactions and observe the evolution of CAPE over them to understand the influence of evaporative controls on convective adjustment.

2 Methods

2.1 Data Sets

2.1.1 Soil Moisture

Soil moisture data used to identify drydowns periods came from the Soil Moisture Active Passive (SMAP) passive microwave radiometer. SMAP Version 7 provides global measurements soil moisture every 2 to 3 days at 36 km resolution (O'Neill et al., 2020). The SMAP satellite was launched in January 2015 and data is available from March 2015 onwards. We use SMAP observations from March 2015 to November 2021 in our study and discarded measurements based on the retrieval quality assessment flag. Measurements discarded include those performed over snow and ice, mountainous topography, open water, urban areas, and vegetation with greater than 5 kg m⁻² water content (Entekhabi et al., 2014).

2.1.2 Meteorological Data

Global temperature, humidity, and pressure data were obtained from the Atmospheric Infrared Sounder (AIRS) instrument (AIRS project, 2019). AIRS Version 7 provides both atmospheric profiles and surface values for the aforementioned variables daily at 1° resolution. The AIRS instrument is mounted atop a polar-orbiting platform (EOS-Aqua) and takes measurements along both its ascending and descending orbits. We use AIRS observations from the ascending orbit, which observes locations at 1:30 PM local time. The length of available AIRS data is much longer than that of SMAP, so we take observations from the time period where SMAP is available.

2.2 Data Processing

2.2.1 CAPE and Moist Enthalpy Calculations

Daily CAPE was calculated for each grid cell using AIRS temperature, humidity, and pressure data. To create the complete atmospheric profile for each variable, we attached surface values to the beginning of the AIRS profile.

We also computed moist enthalpy (ME), defined as the moist static energy at the surface:

$$ME = c_p T + Lq \quad (3)$$

where T is the temperature at the surface, q is the specific humidity at the surface, and c_p and L are constants denoting the specific heat at constant pressure (for dry air) and the latent heat of vaporization, respectively. The first term is the sensible heat contribution, and the second term represents latent heat.

All calculations were performed using the MetPy package in Python (May et al., 2022).

2.2.2 SMAP Regridding

SMAP (36 km) was regridded to the 1° AIRS grid to be able to associate CAPE with soil moisture data for drydown identification. To do this, we considered all available SMAP measurements contained within a 1° AIRS grid cell for every day and computed the area of the grid cell covered by the SMAP swath. If greater than 50% of the total area of the grid cell was observed, the soil

moisture value for that day was determined to be the average of all enclosed SMAP measurements.

2.2.3 Drydown Identification

Fundamentally, drydowns are interstorm periods during which the soil moisture is not strongly affected by precipitation infiltration. Dong et al. (2022) used this working definition of drydowns to develop an algorithm that identifies and removes soil moisture anomalies caused by precipitation—leaving only the drydown time series. We apply that algorithm to the regridded soil moisture time series for each 1° grid cell and take each instance of a drydown to be one “sample.”

Within a drydown sample, days are numbered starting from day $t = 0$ to $n - 1$ (where n is the total length of the drydown), and CAPE and moist enthalpy are saved for each drydown day. We also compute average values of CAPE and moist enthalpy for each day t by averaging across all drydown samples in a grid cell or region.

Figure 1 shows the average (median) drydown length across the globe, computed for each grid cell, as well as the 33rd and 66th percentile values.

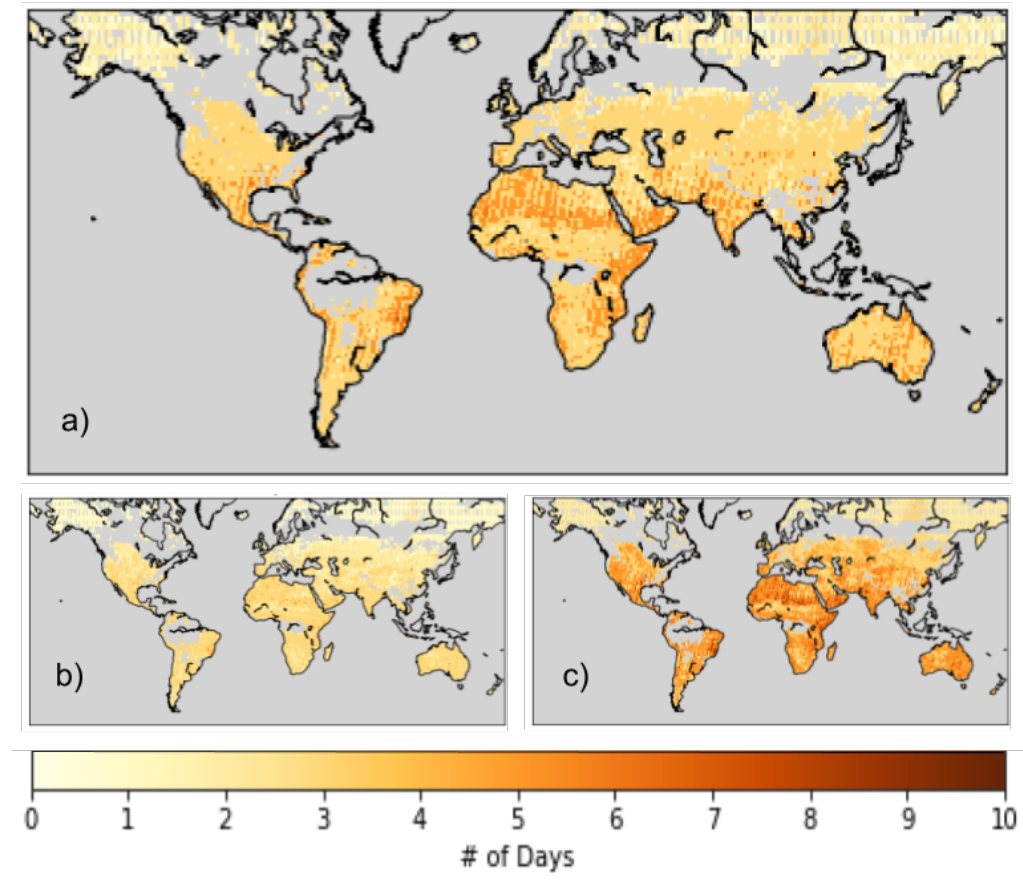


Figure 1. a) Median b) 33rd percentile, and c) 66th percentile drydown length. Gray indicates regions where no drydowns were found, often times due to lack of soil moisture data (see Section 2.1.1).

2.3.4 Warm Season Definition

Drydowns are typically evaluated during summer months (Dong, 2022). In addition, CAPE averages are close to zero in the midlatitudes for the rest of the year. As such, we define a “warm season” for each hemisphere and only evaluate drydowns occurring during the warm season for our analysis of CAPE. The warm season stretches from the month of the summer solstice to the month of the fall equinox (June through September for the Northern Hemisphere and December through March for the Southern Hemisphere).

2.4 Drydown Day Zero Maps

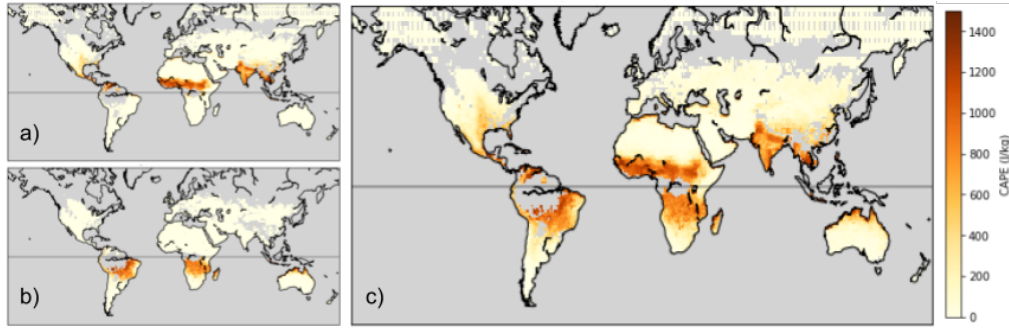


Figure 2. Average initial ($t = 0$) drydown CAPE during a) June-September b) December-March, and c) the warm season (defined in Section 2.3.4).

Figure 2 shows average CAPE values at the beginning of a drydown for the globe. Drydown CAPE differs dramatically across the equator during boreal (Figure 2a) and austral summer (Figure 2b), supporting our decision to define a warm season (Figure 2c) for analysis.

Figure 3 displays average values for moist enthalpy and its components for $t = 0$. Magnitude wise, sensible heat ($c_p T$) is the largest contributor to moist enthalpy. However, we will later see that the sensible heat (Lq) component is the more dominant factor in determining drydown behavior.

In both Figures 2 and 3, drydown CAPE and moist enthalpy data is missing for the areas colored in gray. In most of those regions, drydowns could not be identified due to the lack of high-quality SMAP observations caused by the factors mentioned in Section 2.1.1. Some other regions, such as the East Coast of the United States, are known to not exhibit drydown behavior (Akbar et al., 2018).

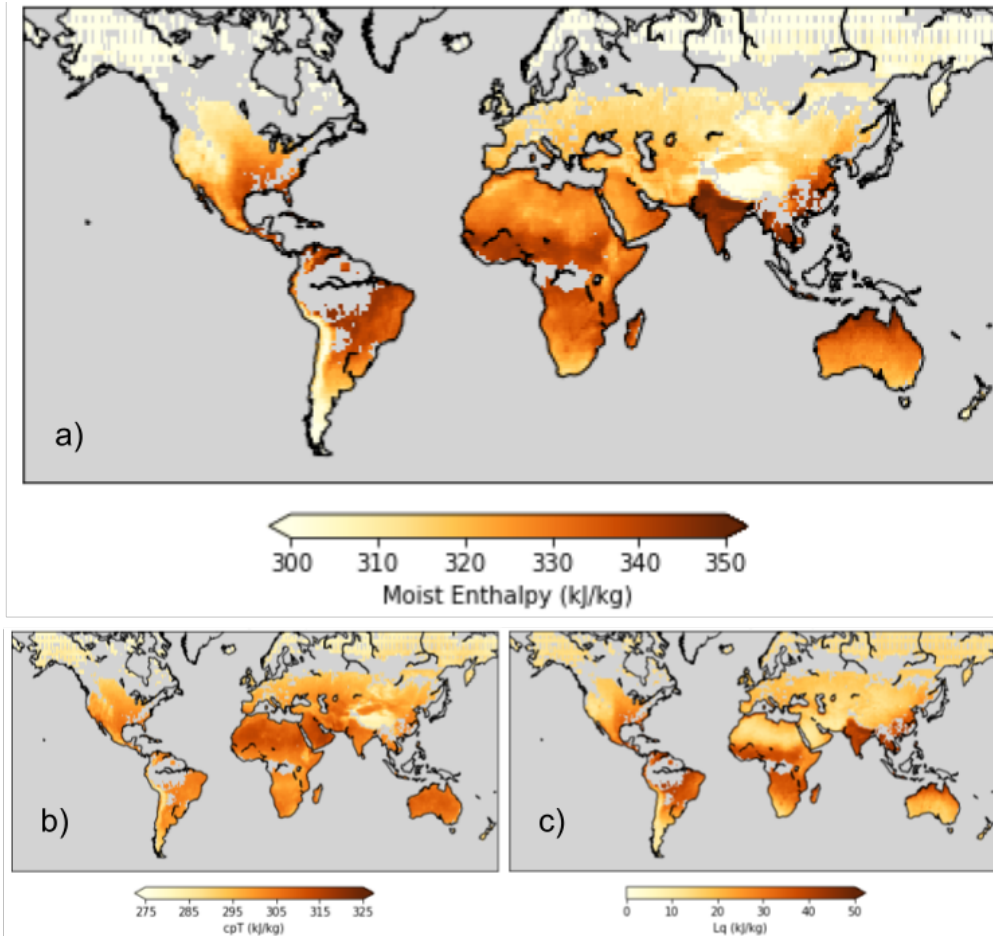


Figure 3. Average initial ($t = 0$) drydown a) moist enthalpy b) sensible heat and c) latent heat across the globe.

3 Continental US Focus Area

3.1 Western and Eastern US Comparison

For our analysis of drydown CAPE behaviors, we first zoomed in on the continental United States (CONUS). The hydroclimatology of the continental US exhibits a strong divide between East and West, a division that can be classified by considering the strongest influence on evaporation in each region. In the arid Western US, low soil moisture content limits evaporation. In so-called “water-limited” regimes, the rate of evaporation is dictated by the amount of water the ground can supply rather than the available radiative energy (Eagleson, 1978; Budyko, 1961). In the Eastern US, where soil moisture is plentiful, evaporation is instead “energy-limited.”

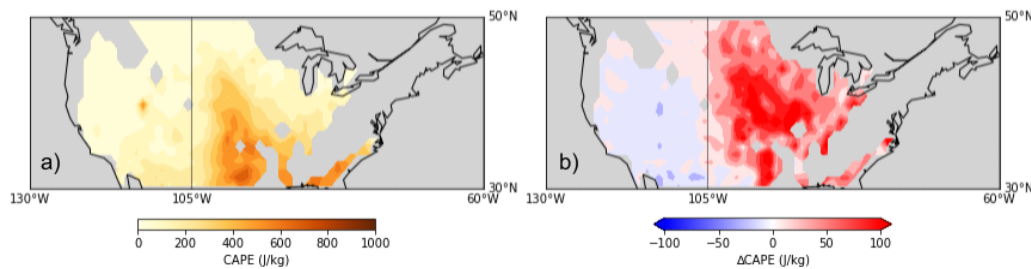


Figure 4. Average a) initial drydown CAPE and b) change in CAPE/day over the continental United States. For our study, “Western US” refers to the area West of the 105°W meridian and “Eastern US” refers to the area East of the marker.

The geographical division between these two regimes is apparent in plots of average initial CAPE and change in CAPE over drydowns (Figure 4). For our analysis, we define the boundary to be at 105°W and compare CAPE behavior during drydowns between the Western and Eastern continental United States.

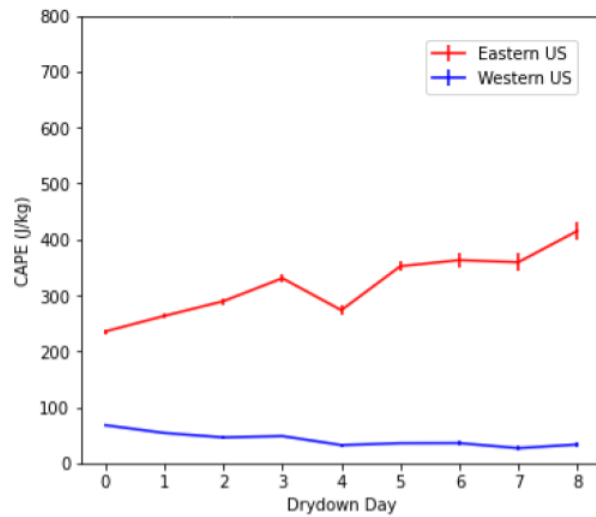


Figure 5. Average CAPE over the course of drydowns in the Eastern (red) and Western (blue) United States.

By averaging CAPE for each day across all drydowns in the Western and Eastern US, we created a drydown time series for CAPE in both regimes (Figure 5). In the Eastern US (red), CAPE increases on average over the course of a drydown. In contrast, the Western US (blue) displays a slight decrease in CAPE as time goes on. Drydown moist enthalpy also exhibits this difference in trends between the two regions (Figure 6b).

We only show drydown behavior up to $t = 8$ because the number of drydown samples becomes too few past nine days, a cutoff that aligns with the drydown time scales found in Figure 1. This decrease in sample size, and the corresponding increase in error, as the drydown goes on is reflected in the error bars of Figure 5, which we do not show for the rest of our analysis.

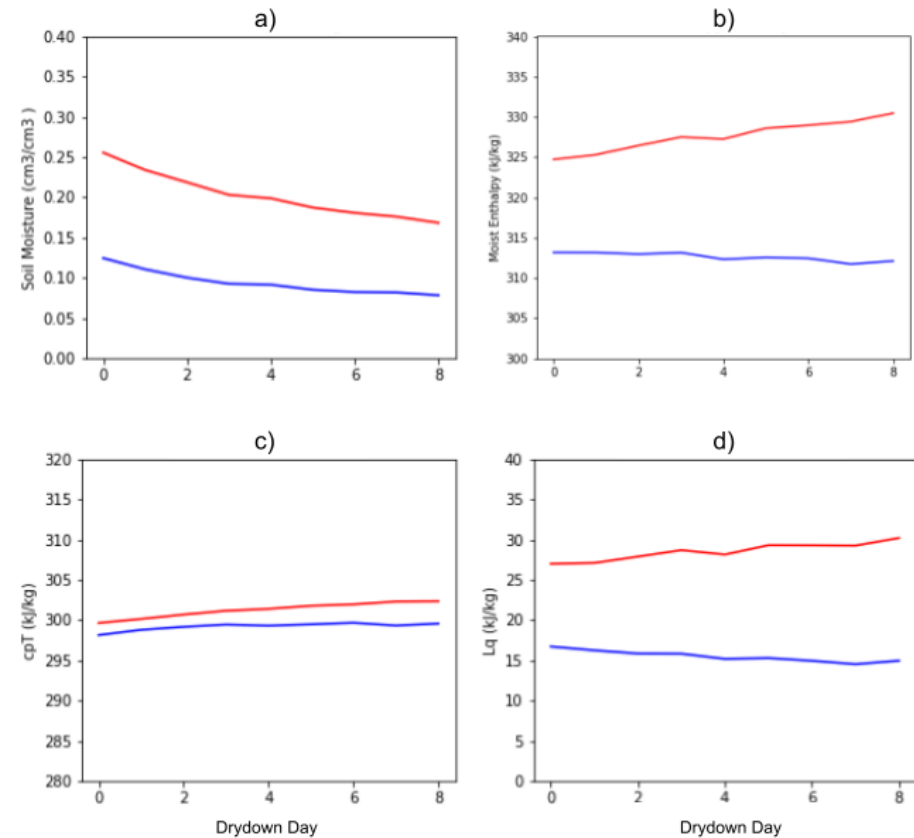


Figure 6. Average a) soil moisture b) moist enthalpy c) sensible heat, and d) latent heat over the course of drydowns in the Eastern (red) and Western (blue) United States.

3.2 “Tagging” by Initial Conditions

We also wanted to understand how CAPE evolution depends on initial conditions at the start of a drydown. To do so, we identified the 33rd and 66th percentile values of initial soil moisture and moist enthalpy over all drydowns in each region and applied a “tag” to drydowns that were either above the 66th percentile or below the 33rd. For example, drydowns with a tag of “sm33” have initial soil moisture values below the 33rd percentile value (i.e., the dry scenario). Conversely, “sm66” denotes drydowns with initial soil moisture values greater than the 66th percentile (i.e., the wettest drydowns).

3.2.1 Initial Soil Moisture Comparison

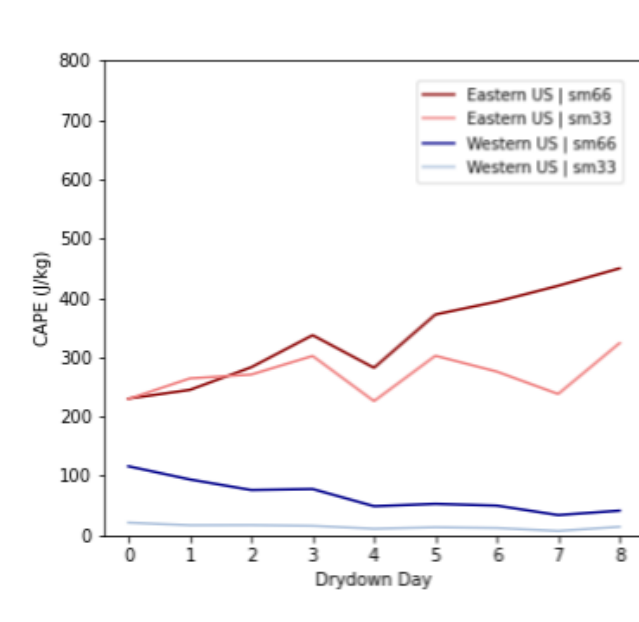


Figure 7. Average CAPE in the Eastern (red) and Western (blue) United States for drydowns in the bottom (light) and top (dark) 33rd percentile of initial soil moisture values.

Figure 7 shows the result of applying soil moisture tags to the drydowns samples in each region. Immediately, we find that the general trends within each region remain the same as in Figure 5 and are distinct from one another; CAPE still increases on average in the East and displays the opposite behavior in the West. Figure 8b shows that these trends are also maintained in drydown moist enthalpy.

In the Western US, drydowns with initial soil moisture above the 66th percentile start out with higher initial CAPE on average and also exhibit a steeper decrease in CAPE over the course of drydowns (Figure 7). Soil moisture also displays a much more prominent decline in the 66th percentile case (Figure 8a). In the East, there is little difference between the two conditions in both the initial and trend in CAPE (Figure 7).

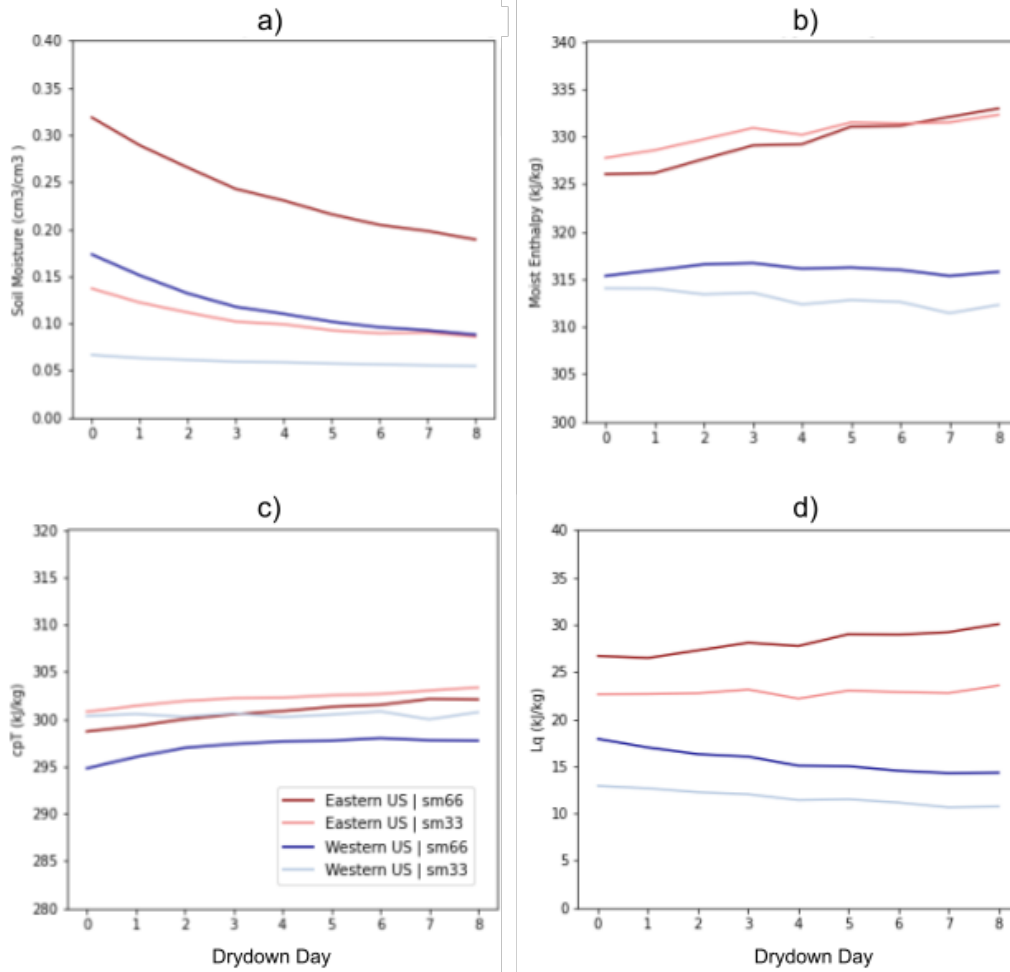


Figure 8. Average a) soil moisture b) moist enthalpy c) sensible heat, and d) latent heat in the Eastern (red) and Western (blue) United States for drydowns in the bottom (light) and top (dark) 33rd percentile of initial soil moisture values.

3.2.2 Initial Moist Enthalpy Comparison

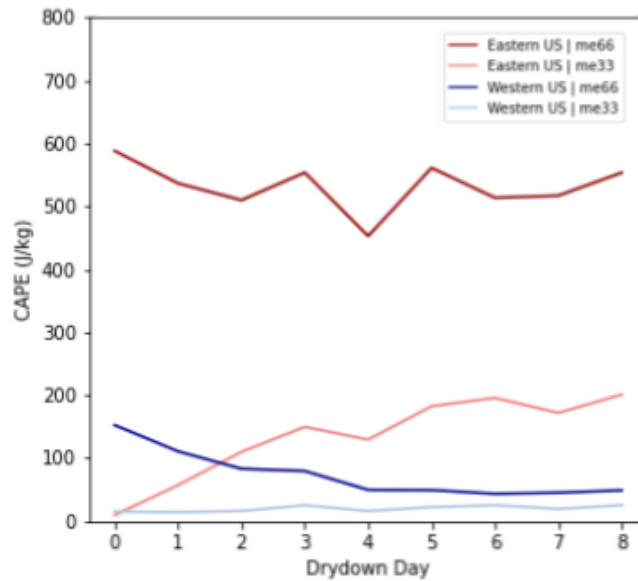


Figure 9. Average CAPE in the Eastern (red) and Western (blue) United States for drydowns in the bottom (light) and top (dark) 33rd percentile of initial moist enthalpy values.

Whereas separating drydowns according to initial soil moisture still maintains the distinction between CAPE evolution in the Western and Eastern US, tagging by initial moist enthalpy produces changes across both regions. In both the Western and Eastern US, CAPE increases when initial moist enthalpy is low and decreases when initial moist enthalpy is high (Figure 9).

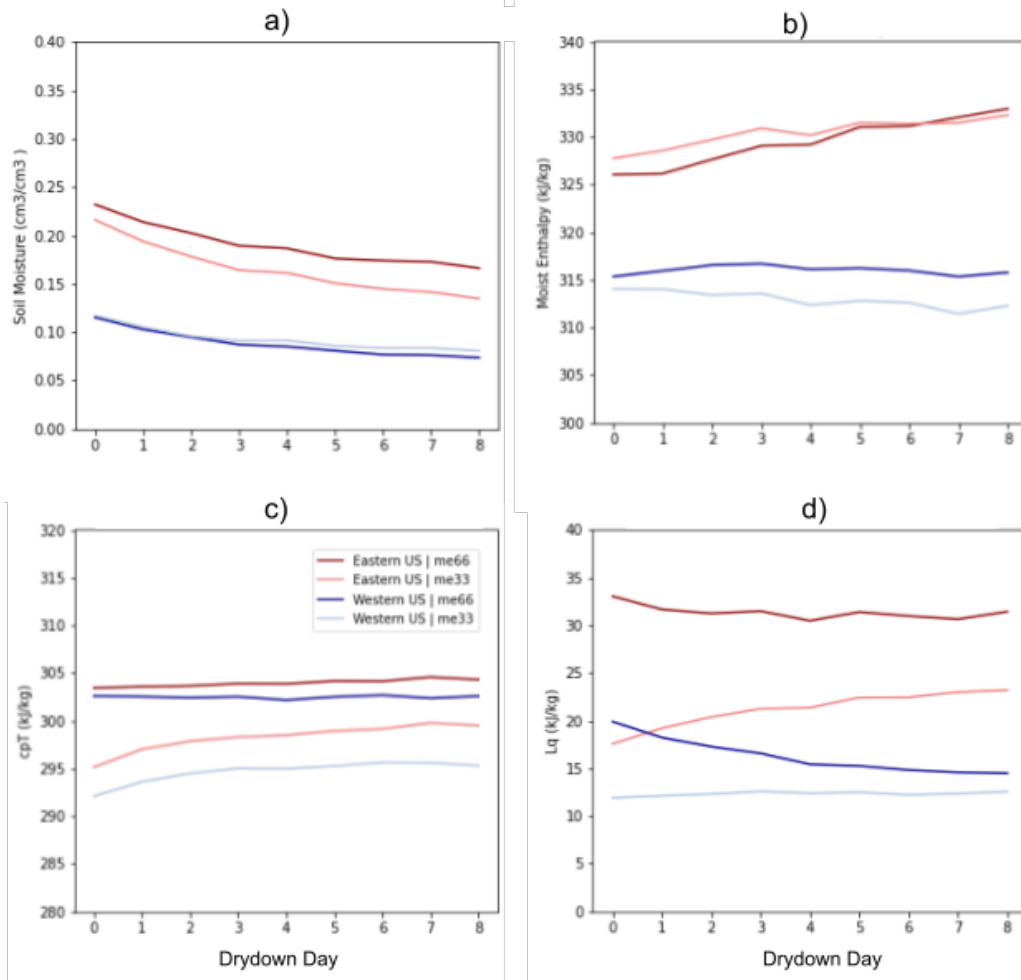


Figure 10. Average a) soil moisture b) moist enthalpy c) sensible heat, and d) latent heat in the Eastern (red) and Western (blue) United States for drydowns in the bottom (light) and top (dark) 33rd percentile of initial moist enthalpy.

When we tag drydown moist enthalpy according to initial values, the same behaviors are clearly displayed (Figure 10b). Moist enthalpy increases over the course a drydown when initially low and decreases when initially high. Breaking moist enthalpy into its components, we find that latent heat most closely matches the direction and magnitude of the aforementioned trends when tagged by initial moist enthalpy (Figure 10d).

3.3 Discussion

Geographical differences in CAPE development between the Western and Eastern United States can be explained by their respective hydroclimates and evaporative regimes. In the Western US, the dry soil quickly runs out of water for evaporation. In the East, however, the moist soil continuously evaporates at the maximum rate dictated by incident radiative energy, leading to greater increases in parcel entropy and CAPE (Equation 2; Figure 5).

Evaporative regimes can also explain the behavior of drydown CAPE under different initial soil moisture conditions. In the Eastern US, where soil moisture is relatively plentiful and thus not the limiting factor for evaporation, there is no difference in CAPE increase between the 33rd and 66th percentile scenarios (Figure 7). Initial soil moisture makes a difference in the Western US because evaporation in the region is determined by the amount of water the soil can supply. As a result, CAPE is higher when the soil contains more moisture, as seen in the 66th percentile scenario (Figure 7). However, the 66th percentile case also exhibits a greater decline in CAPE as the drydown goes on because the amount of evaporation quickly decreases as the soil dries. In the 33rd percentile case, there is little soil moisture and evaporation to begin with, so the time series of both CAPE and soil moisture is relatively flat (Figures 7 and 8a).

Drydown CAPE behavior under different initial moist enthalpy conditions are related to changes in parcel temperature and moisture at the surface, captured by moist enthalpy. Both CAPE and moist enthalpy decrease over the course of a

drydown when initially high and increase when initially low (Figures 9 and 10). When we separated analysis of drydown moist enthalpy into its components, trends in the latent heat component accounted for most of the magnitude of the trends seen in moist enthalpy (Figure 10d). This suggests that changes in the latent heat drive changes in moist enthalpy and CAPE over the course of a drydown, despite it being an order of magnitude smaller than the sensible heat component of moist enthalpy (Figure 3). We explore this phenomenon in greater detail in the following section, where we analyze global drydown behavior.

4 Global Patterns

4.1 Summary Statistics

To form a picture of drydown CAPE over the entire globe, we had to develop statistics that could capture its behavior for a given grid cell. We focus on the change in CAPE per day during drydowns, which we define as:

$$\frac{\Delta \text{CAPE}}{\text{day}} = \text{CAPE}_t - \text{CAPE}_{t-1} \quad (4)$$

In particular, we are interested in whether $\Delta \text{CAPE}/\text{day}$ is positive or negative on average and how often it is positive for a given grid cell. For each grid cell we computed a mean $\Delta \text{CAPE}/\text{day}$ value across all drydown days and a percentage positive statistic that represents the fraction of drydown days that see an increase in CAPE. We also computed the Δ /day for moist enthalpy and its components.

4.2 Results

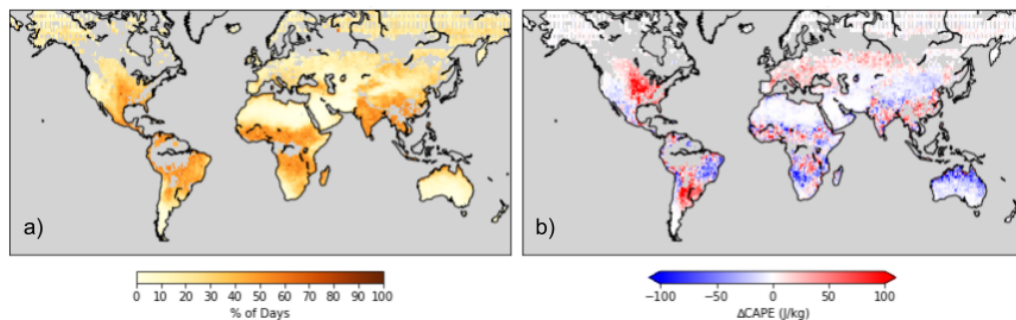


Figure 11. a) Percentage of drydown days with positive $\Delta \text{CAPE}/\text{day}$ and b) mean $\Delta \text{CAPE}/\text{day}$ during drydowns across the globe.

Figure 11 displays summary statistics for $\Delta \text{CAPE}/\text{day}$ over drydowns across the globe. We see that areas where a larger proportion of drydown days see

increases in CAPE correspond to areas with positive $\Delta\text{CAPE}/\text{day}$ values. Over the United States, the Eastern US is red (positive), and the Western US is a faint blue (slightly negative), which aligns with our results in Chapter 3. Outside of the continental US, the Río de La Plata Basin in South America and East Asia also display positive mean $\Delta\text{CAPE}/\text{day}$. Regions such as inland Australia and much of the middle East display negative or close to zero values of $\Delta\text{CAPE}/\text{day}$. The same patterns and hotspots are also found in the $\Delta\text{ME}/\text{day}$ and $\Delta\text{Lq}/\text{day}$ (Figure 12b and 12f).

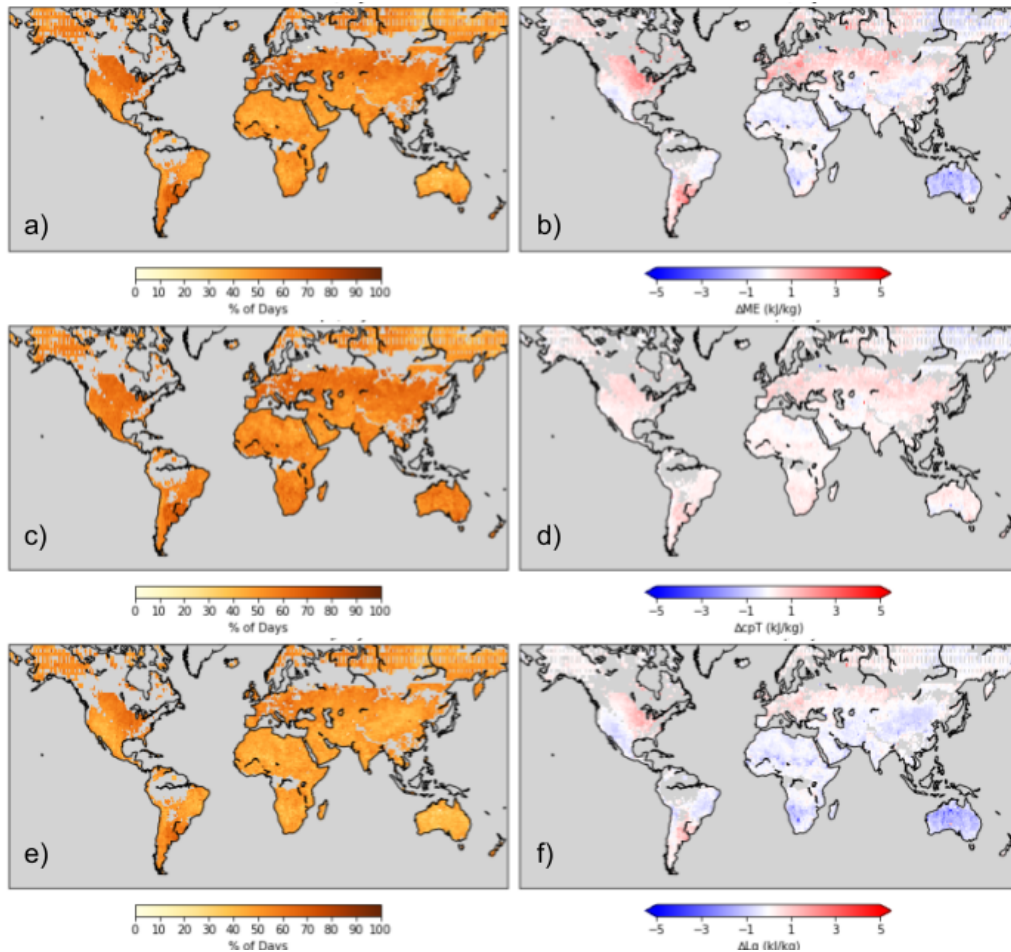


Figure 12. Percentage of drydown days with positive Δ/day (left) and mean Δ/day (right) during drydowns for a-b) moist enthalpy c-d) sensible heat, and e-f) latent heat.

4.2.1 Soil Moisture Tag

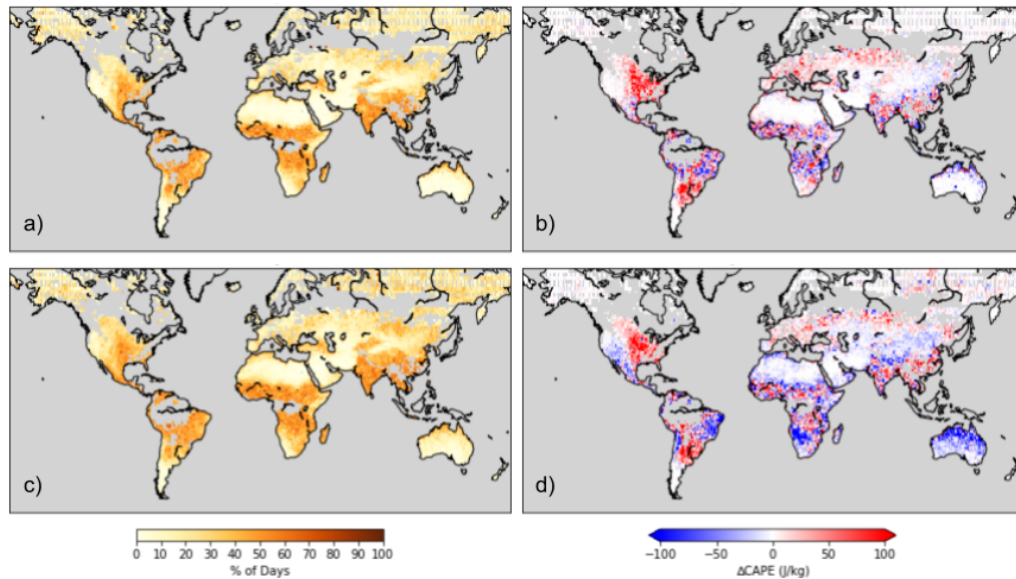


Figure 13. Percentage of drydown days with positive $\Delta\text{CAPE}/\text{day}$ (left) and mean $\Delta\text{CAPE}/\text{day}$ (bottom) for the a-b) bottom 33rd and c-d) top 33rd percentile of initial drydown soil moisture.

Figure 13 shows the result of tagging drydowns within each grid cell by their initial soil moisture values (see Section 3.2). Between the top and bottom 33rd percentile, regions such as the Western US and inland Australia become more negative (blue) in the wetter, 66th percentile case and show little change (white) in the dry 33rd. Once again, these patterns and trends are also seen in the mean ΔME and $\Delta\text{Lq}/\text{day}$.

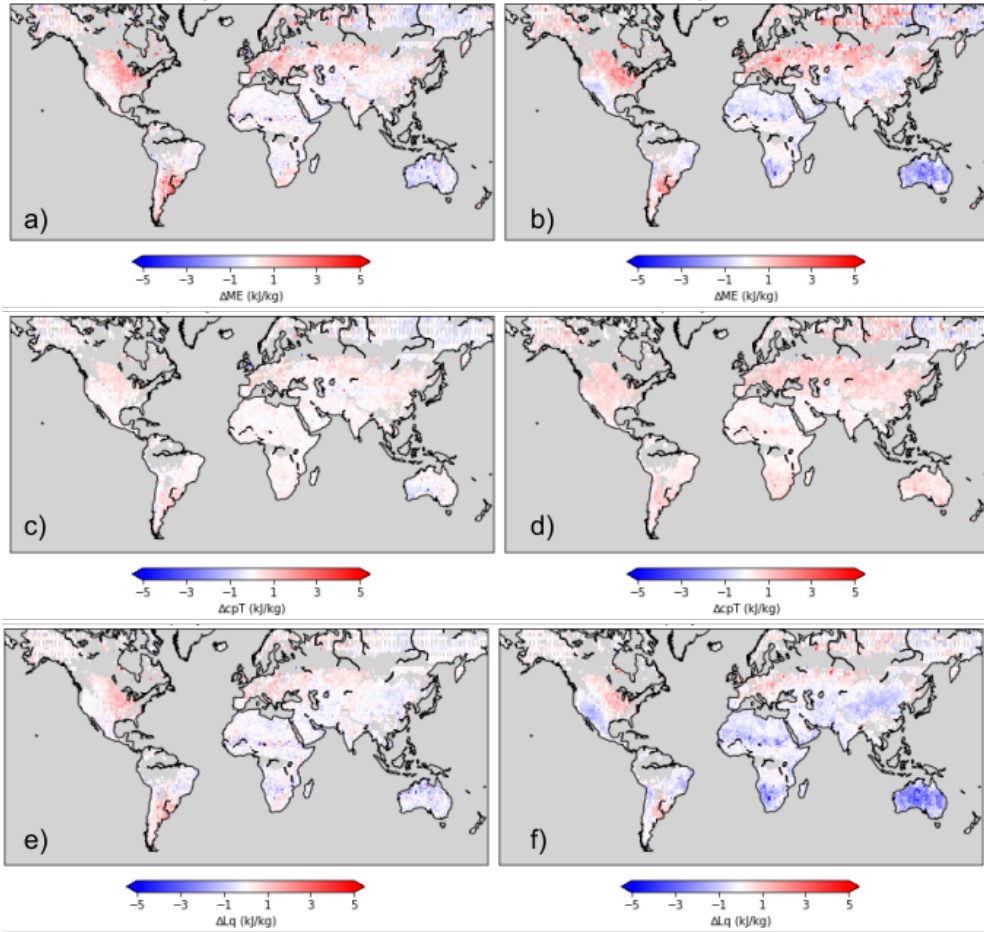


Figure 14. Mean a-b) $\Delta ME/day$ c-d) $\Delta c_p T/day$, and e-f) $\Delta Lq/day$ for the bottom (left side of figure) top (right side of figure) 33rd percentile of initial drydown soil moisture.

4.2.2 Moist Enthalpy Tag

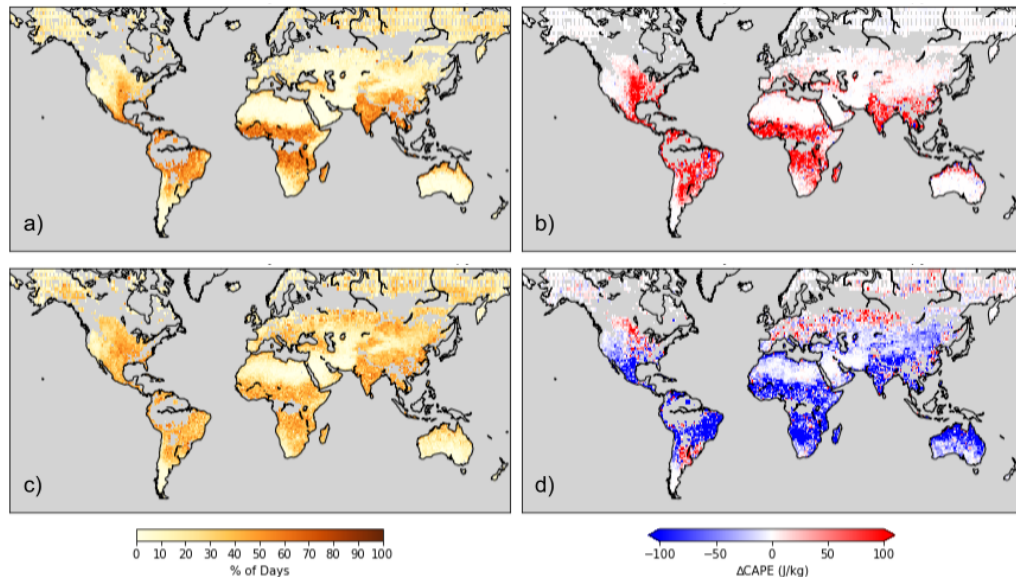


Figure 15. Percentage of drydown days with positive $\Delta\text{CAPE}/\text{day}$ (left) and mean $\Delta\text{CAPE}/\text{day}$ (bottom) for the a-b) bottom 33rd and c-d) top 33rd percentile of initial drydown moist enthalpy.

Unlike soil moisture, the trends in CAPE differ dramatically based on initial moist enthalpy conditions across the globe (Figure 15). When moist enthalpy is initially low, CAPE increases (red) during a drydown. When moist enthalpy is high, CAPE generally decreases (blue) or doesn't change (white)—with some exceptions. The percentage of drydown days where CAPE increases also goes down from the 33rd to the 66th percentile.

Applying the same tag to moist enthalpy itself, this trend manifests even more clearly across the globe (Figure 16a). Between the two components, the latent heat (Figure 16c) mirrors the patterns in moist enthalpy. Sensible heat also displays a difference between the two initial conditions, but to a lesser degree (Figure 16b).

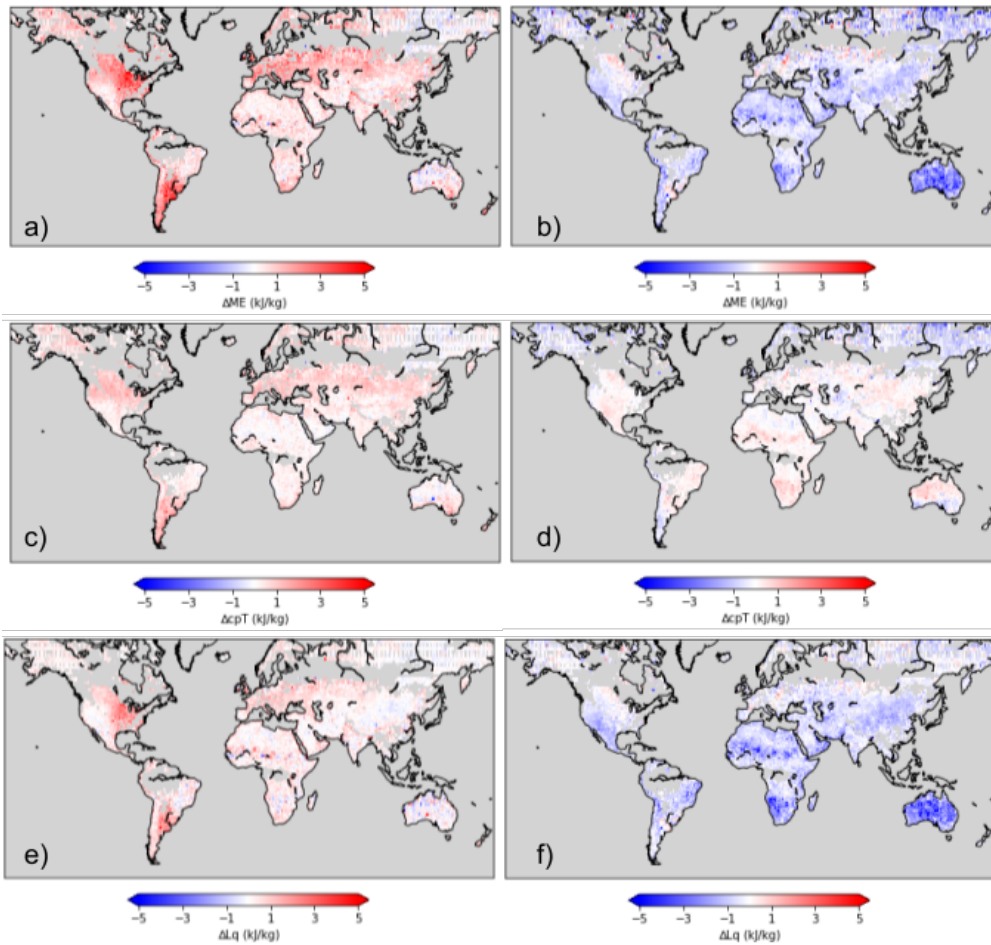


Figure 16. Mean a-b) $\Delta ME/day$ c-d) $\Delta cpT/day$, and e-f) $\Delta Lq/day$ for the bottom (left side of figure) top (right side of figure) 33rd percentile of initial drydown moist enthalpy.

4.2.3 Sensible and Latent Heat Tags

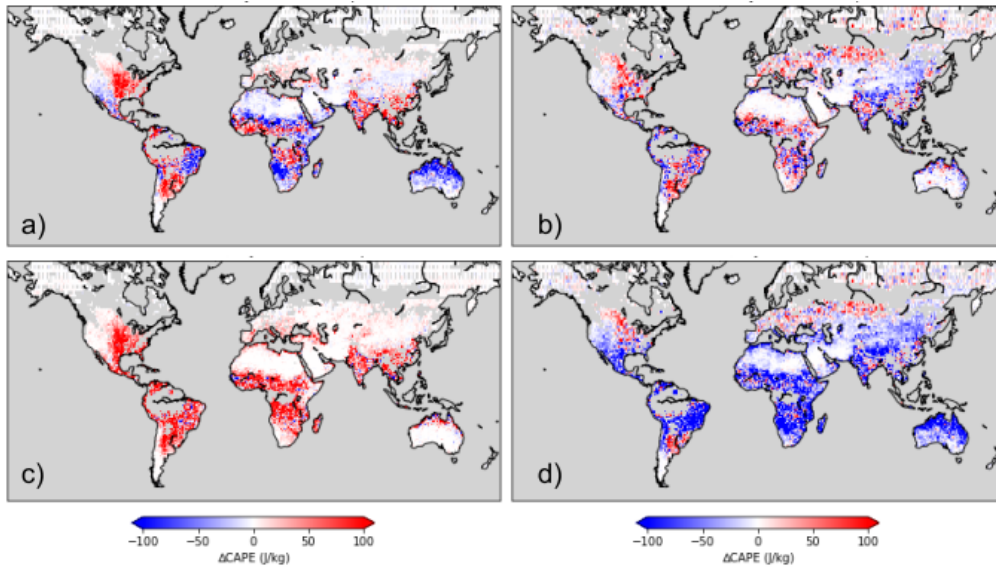


Figure 17. Mean $\Delta\text{CAPE}/\text{day}$ for the bottom (left side of figure) top (right side of figure) 33rd percentile of initial drydown a-b) sensible heat and c-d) latent heat.

Lastly, we tagged CAPE (Figure 17) and moist enthalpy (Figure 18) by both sensible and latent heat to understand which component was the predominant factor in dictating CAPE and moist enthalpy development. The latent heat tag most closely reproduces the patterns seen in the moist enthalpy tag for both ΔCAPE and ΔME .

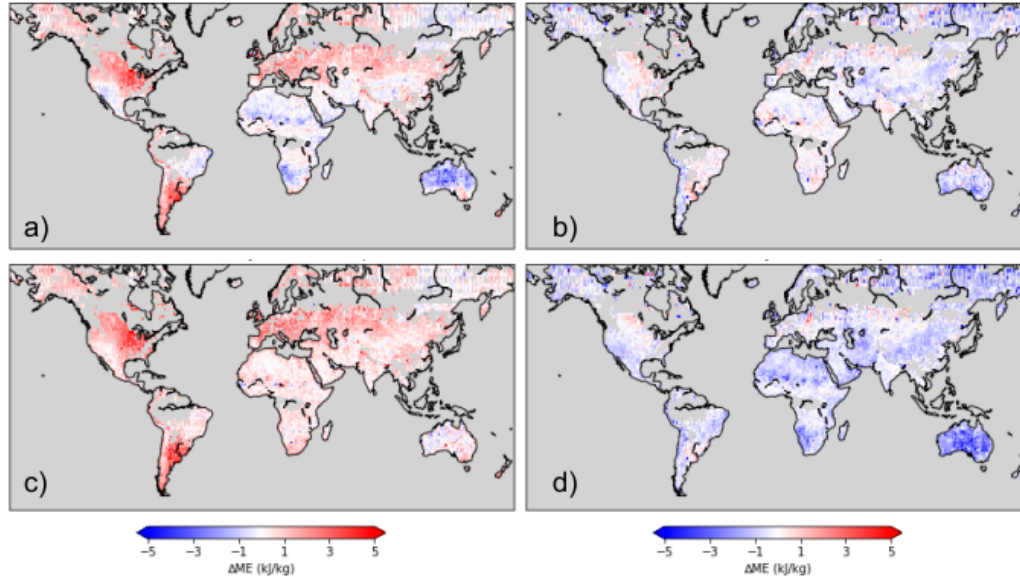


Figure 18. Mean $\Delta ME/day$ for the bottom (left side of figure) top (right side of figure) 33rd percentile of initial drydown a-b) sensible heat and c-d) latent heat.

4.3 Discussion

4.3.1 Geographical Trends

On average, $\Delta CAPE/day$ is positive for humid climates such as the Eastern United States, Río de La Plata Basin, and East Asia (Figure 11b). This suggests that CAPE tends to increase during drydowns over moist surfaces. Since increases in CAPE are driven by evaporation (Equation 1), it follows that the largest increases in CAPE are found over soils that have a lot of water to supply for evaporation.

Conversely, $\Delta CAPE/day$ is on average negative or close to zero in arid regions such as the Western United States, Middle East, and inland Australia (Figure 11b). In these water-limited climates, there is not enough soil moisture to sustain increases in parcel entropy through evaporation. As a result, CAPE decreases or does not change at all over the course of a drydown.

4.3.2 Soil Moisture's Impact

Initial soil moisture conditions had the greatest impact on CAPE evolution in regions where $\Delta\text{CAPE}/\text{day}$ was either negative or zero on average. As noted in the above section, these regions correspond to water-limited regimes where the evaporation rate is dictated by the amount of water the soil can supply. It would make sense then that drydown CAPE is most sensitive to initial soil moisture conditions where evaporation is most sensitive to soil moisture. This is also in line with Koster et al. (2004), who concluded that coupling between evaporation and soil moisture was a necessary condition for coupling between precipitation and soil moisture.

The reason that $\Delta\text{CAPE}/\text{day}$ becomes more negative in arid regions from the 33rd to 66th percentile is because the soil quickly dries out in those regions.

Although CAPE has a higher starting point in the wetter soil (66th percentile) scenario, it decreases more rapidly as the water available for evaporation runs out over time.

4.3.3 Understanding the Moist Enthalpy Tag

In thinking about the impact of initial moist enthalpy on the evolution of CAPE and moist enthalpy itself, our results showed that the latent heat component (and thus humidity) was the key condition. When humidity is high near the surface at the start of a drydown, CAPE, moist enthalpy, and humidity all decrease. This behavior is likely due to the impact of humidity on evaporation.

Across all regions, high humidity limits evaporation; when evaporation is limited, increase in humidity and, consequentially, moist enthalpy and CAPE are also limited. This mechanism produces the global trends we see when considering the impact initial moist enthalpy conditions on CAPE development.

5 Conclusion

Using two global satellite products, we identified soil moisture drydown periods on the surface and evaluated the evolution of CAPE over drydowns. In doing so, we found that the theoretical relationship between CAPE increase and evaporation dictated its drydown behavior.

Geographically, the amount of evaporation and its coupling with initial soil moisture varied across hydroclimates. In humid areas (e.g., Eastern US, South America's Río de La Plata Basin), drydown CAPE increases on average due to high amounts of soil moisture available for evaporation. In drier regions (e.g., Western US, inland Australia), where there is little evaporation, drydown CAPE changes very little on average and may decrease slightly. These regions can also be thought of as water-limited regimes, where evaporation is highly sensitive to soil moisture. As a result, we find that drydown CAPE is also more sensitive to the initial soil moisture in them.

We also analyzed the impact of initial moist enthalpy on drydown CAPE and found that CAPE increases on average when initial moist enthalpy is low and decreases on average when initial moist enthalpy is high. Unlike soil moisture, this behavior manifests across the entire globe. We found that the latent heat component of moist enthalpy was the most important condition in determining this behavior due to the impact of humidity on evaporation.

Overall, we find that evaporation does exert significant control over convective adjustment during interstorm periods. Our results, which are entirely based in observations and basic physical principles, provide a benchmark for understanding the complex near-surface processes that make up land-atmosphere coupling. In particular, the patterns and behaviors we found may be useful in verifying parameterizations of land-atmosphere interactions in Earth system models.

REFERENCES

- AIRS Project (2019). Aqua/AIRS L3 Daily Standard Physical Retrieval (AIRS-only) 1 degree x 1 degree V7.0. Greenbelt, MD, USA. Goddard Earth Sciences Data and Information Services Center (GES DISC).
<https://doi.org/10.5067/UO3Q64CTTS1U>. January 2022.
- Akbar, R., Gianotti, D. J. S., McColl, K. A., Haghghi, E., Salvucci, G. D., & Entekhabi, D. (2018). Estimation of Landscape Soil Water Losses from Satellite Observations of Soil Moisture. *Journal of Hydrometeorology*, *19*(5), 871–889. <https://doi.org/10.1175/JHM-D-17-0200.1>
- Budyko, M. I. (1961). The Heat Balance of the Earth's Surface. *Soviet Geography*, *2*(4), 3–13.
<https://doi.org/10.1080/00385417.1961.10770761>
- Dong, J., Akbar, R., Feldman, A. F., Gianotti, D. J. S., Entekhabi, D. (2022) Land Surfaces at the Tipping-Point for Water and Energy Balance Coupling. *Water Resources Research*. under review
- Eagleson, P. S. (1978). Climate, soil, and vegetation: 4. The expected value of annual evapotranspiration. *Water Resources Research*, *14*(5), 731–739.
<https://doi.org/10.1029/WR014i005p00731>
- Entekhabi, D., Yueh, S., O'Neill, P. E., Kellogg, K. H., Allen, A., Bindlish, R., Brown, M., Chan, S., Colliander, A., Crow, W. T., Das, N., De Lannoy, G., Dunbar, R. S., Edelstein, W. N., Entin, J. K., Escobar, V., Goodman, S. D., Jackson, T. J., Jai, B., ... West, R. (2014). *SMAP Handbook—Soil Moisture Active Passive: Mapping Soil Moisture and Freeze/Thaw from*

- Space*. JPL Publication; Pasadena, CA.
- <https://lirias.kuleuven.be/retrieve/365384>
- Koster, R. D., Dirmeyer, P. A., Guo, Z., Bonan, G., Chan, E., Cox, P., Gordon, C. T., Kanae, S., Kowalczyk, E., Lawrence, D., Liu, P., Lu, C.-H., Malyshev, S., McAvaney, B., Mitchell, K., Mocko, D., Oki, T., Oleson, K., Pitman, A., ... Yamada, T. (2004). Regions of Strong Coupling Between Soil Moisture and Precipitation. *Science*, *305*(5687), 1138–1140. <https://doi.org/10.1126/science.1100217>
- May, R. M., Arms, S. C., Marsh, P., Bruning, E., Leeman, J. R., Goebbert, K., Thielen, J. E., Bruick, Z., and Camron, M. D. (2022). MetPy: A Python Package for Meteorological Data. <https://doi.org/10.5065/D6WW7G29>.
- McColl, K. A., Wang, W., Peng, B., Akbar, R., Short Gianotti, D. J., Lu, H., Pan, M., & Entekhabi, D. (2017). Global characterization of surface soil moisture drydowns. *Geophysical Research Letters*, *44*(8), hh. <https://doi.org/10.1002/2017GL072819>
- O'Neill, P. E., S. Chan, E. G. Njoku, T. Jackson, R. Bindlish, and J. Chaubell. (2020). SMAP L3 Radiometer Global Daily 36 km EASE-Grid Soil Moisture, Version 7. Boulder, Colorado USA. NASA National Snow and Ice Data Center Distributed Active Archive Center. <https://doi.org/10.5067/HH4SZ2PXSP6A>. January 2022.
- Salvucci, G. D., Saleem, J. A., & Kaufmann, R. (2002). Investigating soil moisture feedbacks on precipitation with tests of Granger causality.

Advances in Water Resources, 25(8–12), 1305–1312.

[https://doi.org/10.1016/S0309-1708\(02\)00057-X](https://doi.org/10.1016/S0309-1708(02)00057-X)

Seneviratne, S. I., Corti, T., Davin, E. L., Hirschi, M., Jaeger, E. B., Lehner, I.,

Orlowsky, B., & Teuling, A. J. (2010). Investigating soil moisture–
climate interactions in a changing climate: A review. *Earth-Science
Reviews*, 99(3–4), 125–161.

<https://doi.org/10.1016/j.earscirev.2010.02.004>

Tuttle, S., & Salvucci, G. (2016). Empirical evidence of contrasting soil

moisture–precipitation feedbacks across the United States. *Science*,
352(6287), 825–828. <https://doi.org/10.1126/science.aaa7185>